J. Fluid Mech. (2012), *vol.* 700, *pp.* 502–513.
doi:10.1017/jfm.2012.157

Hydraulic control of continuously stratified flow over an obstacle

Kraig B. Winters† and Laurence Armi

Scripps Institution of Oceanography and Mechanical and Aerospace Engineering, University of California San Diego, La Jolla, CA 92093, USA

(Received 11 January 2012; revised 13 March 2012; accepted 23 March 2012; first published online 18 April 2012)

Motivated by the laboratory experiments of Browand & Winant (*Geophys. Fluid Dyn.*, vol. 4, 1972, pp. 29–53), a series of two-dimensional numerical simulations of flow past a cylinder of diameter d are run for different values of the approach Froude number $Fr_o = U/Nd$ between 0.02 and 0.2 at $Re = O(100)$. The observed flow is characterized by blocking and upstream influence in front of the cylinder and by relatively thin, fast jets over the top and bottom of the cylinder. This continuously stratified flow can be understood in terms of an inviscid non-diffusive integral inertia–buoyancy balance reminiscent of reduced-gravity single-layer hydraulics, but one where the reduced gravity is coupled to the thickness of the jets. The proposed theoretical framework describes the flow upstream of the obstacle and at its crest. The most important elements of the theory are the inclusion of upstream influence in the form of blocked flow within an energetically constrained depth range and the recognition that the flow well above and well below the active, accelerated layers is dynamically uncoupled. These constraints determine, through continuity, the transport in the accelerated layers. Combining these results with the observation that the flow is asymmetric around the cylinder, i.e. hydraulically controlled, allows us to determine the active layer thicknesses, the effective reduced gravity and thus all of the integral flow properties of the fast layers in good agreement with the numerically computed flows.

Key words: hydraulic control, stratified flows, topographic effects

1. Introduction

We consider the two-dimensional stratified flow around a cylinder towed perpendicular to both its axis of symmetry and gravity in a uniformly stratified fluid as in Browand & Winant (1972). Although the geometry is deceptively simple, and flow around cylinders has been studied for more than a century, the addition of strong stratification to this problem provides a simple setting in which the fundamental processes of stratified flow over topography can be studied. In particular, the effects of blocking, upstream influence, topographic control and intensified downslope flow are all exhibited and can be related to the external parameters.

If we take the ambient fluid to be unbounded, the flow is characterized by three external scales: the squared buoyancy frequency $N^2 = (g/\rho_0)(\mathrm{d}\bar{\rho}/\mathrm{d}z)$, the speed of

† Email address for correspondence: kraig@coast.ucsd.edu

the cylinder U and its diameter d. These parameters can be combined to form the bulk Froude number $Fr_o = U/Nd$ which can be interpreted as the ratio of the vertical displacement scale $\delta = U/N$ to the cylinder diameter d. Vertical displacements of $O(\delta)$ require complete conversion from kinetic to potential energy of fluid parcels moving with a speed U. When $Fr_o \ll 1$, the regime of interest here is $Fr_o = O(10^{-2}–10^{-1})$, buoyancy acts to inhibit vertical motions larger than $\delta \ll d$ and so most of the fluid upstream of the cylinder has insufficient kinetic energy to be lifted over or pushed under the cylinder 'crests' and can therefore be expected to be blocked. Equivalently, as in Browand & Winant (1972), these parameters can be combined to form a bulk Richardson number $Ri_0 = 1/Fr^2$.

In addition to N^2, U and d, the fluid properties ν and κ, the diffusivity of momentum and the stratifying agent respectively, also influence the flow and these effects are characterized by the Reynolds number $Re = Ud/\nu$ and the Prandtl number $Pr = \nu/\kappa$. In this work, we will consider flows with $Re = O(100)$ and $Pr = 7$. Unstratified flow around a cylinder at comparable Re exhibits unsteadiness due to the shedding of the vortices in the von Karmen vortex street. In Browand & Winant (1972) and in the present numerical study, strong stratification suppresses the vortex shedding and the flow is symmetric about the horizontal midplane.

2. Numerical experiments

In the experiments of Browand & Winant (1972), cylinders with diameters ranging from 6.5 to 44.5 mm were towed at a speed of a few millimetres per second through a long shallow tank 8.5 m (28 ft) × 0.38 m (15 in) depth × 0.3 m (12 in) width of approximately uniformly salt-stratified fluid by means of thin cables. After the cylinders had been towed a distance of 20–30d, vertical profiles of horizontal velocity (via displacement of dye lines) and density (profiling probe) were obtained repeatedly at a fixed upstream station. Assuming the flow to be steady, such measurements yielded velocity and density profiles as a function of distance from the advancing cylinder.

We adopt a similar approach in the numerical experiments and compute the flow around a moving cylinder within a two-dimensional tank of matching dimensions. We take $d = 44.5$ mm and a tow speed of 2.04 mm s^{-1} which gives $Re = 91$ for $\nu = 10^{-6}$ m^2 s^{-1}. We then vary the buoyancy frequency N across experiments yielding a range of bulk Froude numbers. We report here on simulations with $Fr_o = 0.02, 0.04, 0.1$ and 0.2.

The flows were computed using a spectral numerical model which is an upgraded version of that discussed in Winters, MacKinnon & Mills (2004) and Echeverri *et al.* (2009). Dependent variables are expanded in even or odd Fourier series such that free-slip, no-scalar flux conditions are satisfied at the bottom and sidewalls by each basis function in the expansions. In addition, no-slip, no scalar flux boundary conditions are imposed on the immersed boundary of a cylinder (circle in two dimensions) moving horizontally at speed U. The cylinder is translated a distance of 35d at which point the flow is nearly steady and the flow field is analysed. All simulations reported were computed on a grid of 9601 × 601 points in the x (streamwise) and z (vertical) directions which corresponds to grid spacings of 0.88 and 0.64 mm, respectively.

3. Overview of results

Figure 1 shows snapshots of the flow field after the cylinder has been translated a distance of 35d. Although the solutions were computed for the full cylinder, we only

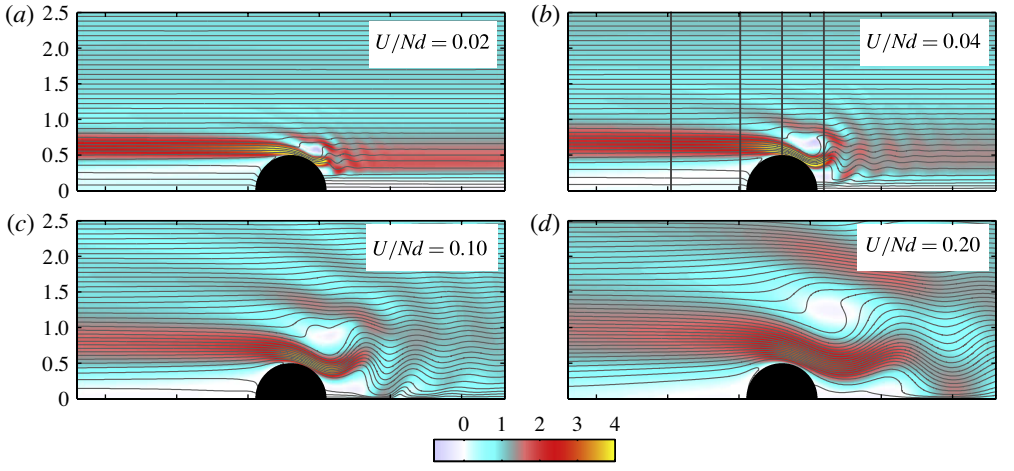

FIGURE 1. Flow above the horizontal centreplane for four values of $Fr_o = U/Nd$ at time $t = 35d/U$. The horizontal speed of the fluid relative to the moving cylinder, normalized by U, is shown in colour along with several isopycnals. Also shown in (*b*) are the four locations of the vertical velocity profiles shown in figure 2. Jets that accelerate, thin and plunge over the cylinder crest are apparent in all four figures.

show the upper half plane since the solutions were observed to be symmetric, as also seen in the photographs of Browand & Winant (1972). In the figure, the normalized relative velocity $(u(x, z) - U)/U$ is shown in colour. Also shown are several isopycnals. Several qualitative features of the flow are apparent in all four figures: there is a depth limited, relatively fast flowing jet that extends from upstream above the cylinder crest that thins, accelerates and plunges near the crest of the cylinder. Upstream and below this jet, the fluid is arrested or nearly arrested in a frame moving with the cylinder. Upstream and above this jet, the flow is nearly uniform and approaches the cylinder at the translation speed U. Above the jet and slightly downstream (to the right) of the cylinder crest, there is a slug of nearly stagnant fluid with nearly uniform density. These jets detach from the cylinder in the lee and exhibit vertical oscillations further downstream. The upstream–downstream asymmetry in the vertical position of the accelerated jet relative to the cylinder crest is reminiscent and strongly suggestive of some form of internal hydraulic control and motivates much of the theoretical framework discussed in § 4.

Figure 2 shows vertical profiles of horizontal velocity u (relative to the cylinder and normalized by U) at the four locations shown in the upper right of figure 1. Approaching the cylinder ($x/d = -1.50$), the profile exhibits an accelerated jet extending from just below the maximum cylinder height to about $z/d = 1$ with a peak speed of slightly greater than $2U$. Below this layer the fluid is blocked and stagnant, while above the flow is nearly uniform with speed U. We refer to the flow aloft at speed U as 'dynamically uncoupled'. Just in front of the cylinder ($x/d = -0.56$), the profile is similar except the block region is slightly thicker while the jet is slightly thinner and significantly faster. Over the cylinder crest ($x/d = 0$), the jet is both significantly thinner and faster still. Just above the jet, there is a slow moving layer (labelled stagnant) with a minimum velocity of nearly zero. This slow moving fluid is more pronounced in the profile slightly downstream of the cylinder. Qualitatively similar descriptions apply to each of the other flows shown in figure 1. Moreover,

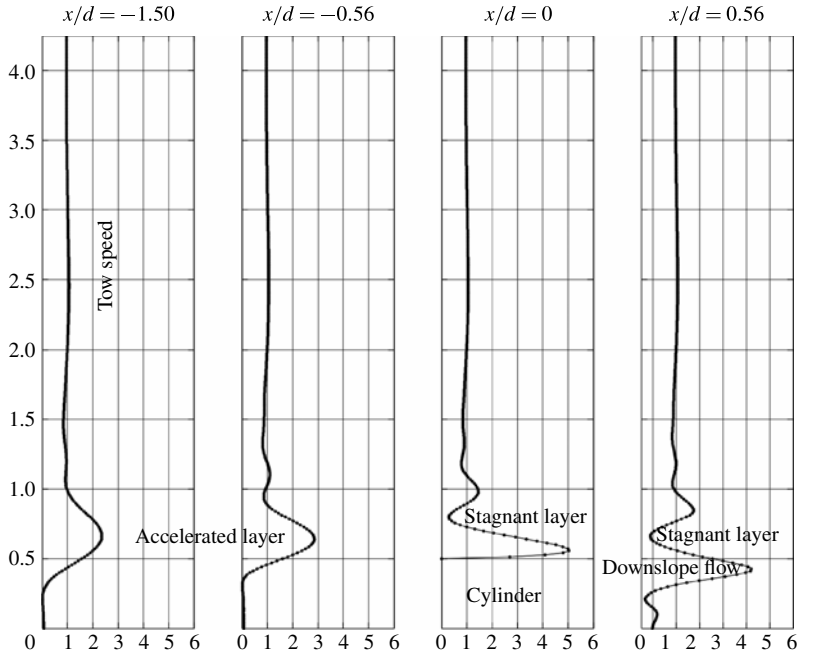

FIGURE 2. Vertical profiles of horizontal velocity relative to the cylinder and normalized by U for $Fr_o = 0.04$. The profile locations are indicated in figure 1(*b*).

these features are ubiquitous signatures of low-Froude-number flow over topography (Baines 1995).

4. Theoretical framework

We now construct a theory to try to explain or predict (*a*) the density range and upstream thickness of the accelerated jets and (*b*) the thickness and speed of the jets as they pass over the crest of the obstacle. In constructing the theory, we exploit the observed symmetry about the horizontal midplane. We adopt a reference frame in which the cylinder is fixed and the flow is from left to right, focusing on the flow upstream of the cylinder crest and we ignore from the outset viscous and diffusive effects.

To begin, we appeal to energetics and argue that the flow is blocked from the midplane to a height $d/2 - \delta$ where $\delta = U/N$. Note that δ is the vertical displacement with a potential energy change matching the kinetic energy of the tow speed U in stratification N. By symmetry, the flow beneath the cylinder is identical and from now on we focus our discussion on the upper portion of the flow.

Above the blocked region, we assume there is an 'active' layer of accelerated fluid with as yet unknown vertical thickness $y(x)$, unknown horizontal speed $u(x) > U$ and unknown average density ρ. The transport q in the active layer is an unknown constant.

Further above is a 'dynamically uncoupled' layer with speed U. Separating these flowing layers is a stagnant layer whose thickness increases as the lower layer thins approaching the obstacle crest. This layer, defined by a bifurcating isopycnal and streamline, also appears in the theory of severe downslope winds (Smith 1985; Durran

& Klemp 1987), although we generalize these earlier theories here by incorporating the effect of blocking upstream of the obstacle. We assume the stagnant layer has infinitesimal thickness well upstream of the cylinder. (We denote 'well upstream' here as x_{us} even though in the truly far field we implicitly assume uniform flow approaching the cylinder.) The as yet unknown mean densities in the active and stagnant layers can be combined to yield a reduced gravity $g' = (\Delta\rho/\rho_0)g$.

The theory will link the layer thickness y, the density difference $\Delta\rho$ and the active layer speed u with the external parameters. We remark that the distance between the cylinder crest and the upper rigid lid does not enter into the analysis. The elements of this theoretical framework are qualitatively consistent with the flows shown in figures 1 and 2.

We adopt an integral approach for the characteristic values of the velocity and density. In taking this approach, we sacrifice details such as the distribution of velocity and density within the active layer in favour of retaining the fundamental nonlinearity of the flow. Algebraically, what follows is reminiscent of reduced gravity single layer hydraulics. What is new here is that g' is coupled to the upstream layer thickness y and that the layer transport q is determined by the extent of the blocked layer.

The key elements in the theory will be an inertia–buoyancy balance in the absence of friction, and recognition that the flow over the cylinder crest is asymmetric and thus hydraulically controlled. This is entirely different from the small-Reynolds-number viscous–buoyancy balance of Graebel (1969) to which Browand & Winant (1972) compared their measurements. In our experiments and in those of Browand and Winant, the Re is $O(100)$ and inertial effects dominate viscous effects in the regions of interest. Assuming hydrostatic pressure, the dimensional momentum equation for the active layer can be written as

$$uu_x + g'y_x = -g'h_x \tag{4.1}$$

or

$$[u^2/2 + g'(y+h)] = B \tag{4.2}$$

where u is the characteristic speed of the layer and B is the layer Bernoulli constant. Both forms of the equation will be needed in what follows.

The continuity equation can also be written in two forms

$$(uy)_x = uy_x + yu_x = 0 \Rightarrow u_x = -uy_x/y \tag{4.3}$$

or

$$uy = q. \tag{4.4}$$

These are simply the equations for reduced gravity single-layer hydraulics but, in addition to B and q, g' is now to be determined. We note that solutions for the integrated quantities, i.e. u and g', are not particularly sensitive to the functional form within layers, e.g. Armi (1989). A similar integral approach for continuously stratified flow through a contracting channel was taken by Wood (1968) who was able to construct exact, self-similar solutions.

Substituting the expression for u_x from (4.3) into (4.1) and solving for y_x gives

$$y_x = -\frac{h_x}{1 - F^2} \tag{4.5}$$

where $F^2(x) = u^2/g'y$ is the square of the layer Froude number. Equation (4.5) implies that y_x is finite everywhere provided that $F \neq 1$. If $F = 1$ somewhere, y_x can remain

finite only if $h_x = 0$. This regularity condition says that critical flow can only occur at the crest of the cylinder. A finite value $|y_x| > 0$ at the cylinder crest x_c therefore implies asymmetric flow across the crest that is hydraulically controlled. Note that the active layers in figure 1 are thinning as they crest the cylinder with thickness, height and speed of the layers being asymmetric across the crest.

Denoting conditions at the cylinder crest with the subscript c, the requirement that $F_c = 1$ can be combined with (4.2) to give an expression for the layer thickness at the crest y_c:

$$y_c = \tfrac{2}{3}(B/g' - h_c). \tag{4.6}$$

Combining continuity equation (4.4) with (4.2) and evaluating the result at the crest yields

$$\frac{1}{2}\frac{q^2}{y_c^2} + g' y_c = B - g' h_c. \tag{4.7}$$

The quantity $B - g'h(x)$ is often referred to as the specific energy $\mathscr{E}$ of the layer.

At this point it is convenient to non-dimensionalize (4.6) and (4.7) using the (still unknown) quantities q and g' as in Pratt & Whitehead (2008). Taking $h = q^{2/3}g'^{-1/3}\tilde{h}$ and $B = q^{2/3}g'^{2/3}\tilde{B}$, where the tildes indicate dimensionless variables, equations (4.6) and (4.7) give two expressions for the dimensionless specific energy $\tilde{\mathscr{E}}_c$ at the crest:

$$\tilde{\mathscr{E}}_c = (\tilde{B} - \tilde{h}_c) = \frac{3}{2}\tilde{y}_c \quad \text{and} \quad \tilde{\mathscr{E}}_c = (\tilde{B} - \tilde{h}_c) = \frac{1}{2\tilde{y}_c} + \tilde{y}_c. \tag{4.8}$$

Eliminating $\tilde{\mathscr{E}}_c$ and taking the positive root of the resulting quadratic for $\tilde{y}_c$ gives $\tilde{y}_c = 1$ and, upon substitution, $\tilde{\mathscr{E}}_c = 3/2$ as requirements for the dimensionless layer thickness and specific energy at the crest for hydraulically controlled, asymmetric flow in an active layer. We now use these constraints to derive the values for the unknowns g', q and B from which we can obtain our originally desired quantities, the layer thickness and flow speed at the crest.

The calculation proceeds as follows. Begin by guessing a value for the upstream layer thickness y_{us} (see figure 3). Taking N constant, the unperturbed density is linear in z. Assuming that the density of the stagnant layer is equal to the density at the top of the active layer, i.e. that the stagnant layer has infinitesimal thickness upstream, the difference between the mean density in the active layer and the stagnant layer is $\Delta\rho = (\rho_0/2g)N^2 y_{us}$. The value of g' for such a layer is then $g\Delta\rho/\rho_0$.

We now assume that the bottom of this layer sits at height $d/2 - \delta$, i.e. above the zone of blocked flow. Since we postulate dynamically uncoupled flow with speed U above and depth-independent flow at speed U in the far field upstream, the transport $q = y_{us}u_{us}$ in the active layer must, from continuity, be equal to $U(h_{us} + y_{us})$ where $h_{us} = h_c - \delta = d/2 - U/N$. This yields expressions for the upstream velocity and the upstream Froude number:

$$u_{us} = \frac{h_{us} + y_{us}}{y_{us}} U > U \quad \text{and} \quad F_{us} = \frac{u_{us}}{g' y_{us}}. \tag{4.9}$$

With these values, we can now compute the Bernoulli constant for our hypothetical active layer: $B = (1/2)u_{us}^2 + g'(h_{us} + y_{us})$.

Given B, g' and q, we can now non-dimensionalize as before and compute the normalized specific energy at the crest $\tilde{\mathscr{E}}_c(y_{us}) = (\tilde{B} - \tilde{h}_c)$. Had we prescribed the value

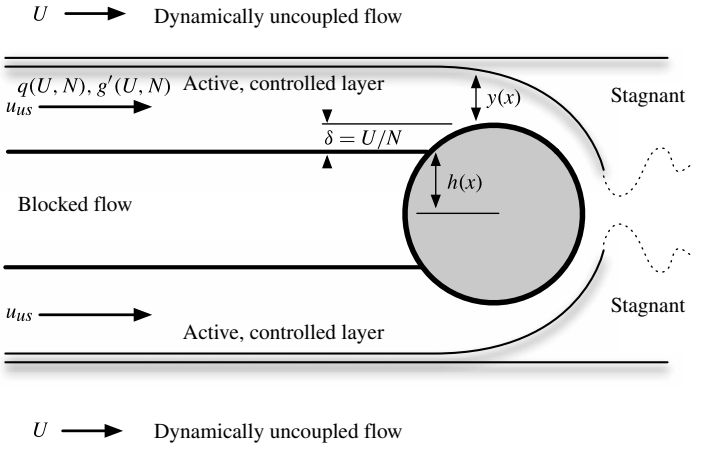

FIGURE 3. Schematic of stratified flow around a towed cylinder moving from right to left. Shown are two active layers, one above and one below and a central region of blocked flow. Each of the active layers is bounded by stagnant flow. Well above and below the cylinder, the flow is dynamically uncoupled and has speed U relative to the towed cylinder. The active layer is treated as a single-layer hydraulically controlled flow with q and g' functions of U and N. Here $h(x)$ is the distance from the horizontal midplane to the 'virtual topography' which extends from the cylinder itself upstream along the boundary of the blocked flow.

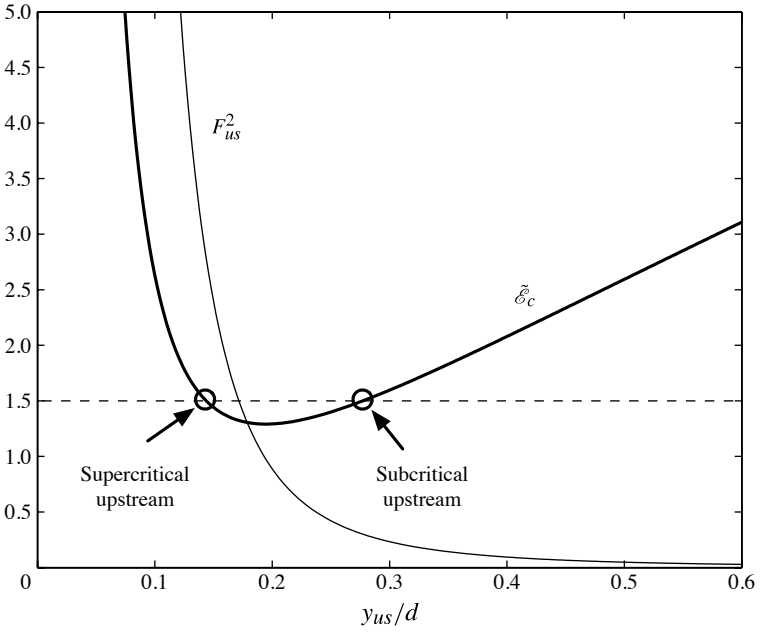

FIGURE 4. Normalized specific energy $\tilde{\mathscr{E}}_c$ at the cylinder 'crest' as a function of y_{us} and the corresponding value of the upstream Froude number F_{us} for the specific case $Fr_o = 0.04$.

of y_{us} correctly at the start of the calculation, we would find that $\tilde{\mathscr{E}}_c(y_{us}) = 3/2$, our requirement for controlled, asymmetric flow. We can repeat the procedure, varying our guess for y_{us}, until we find the value that satisfies the requirement for controlled flow.

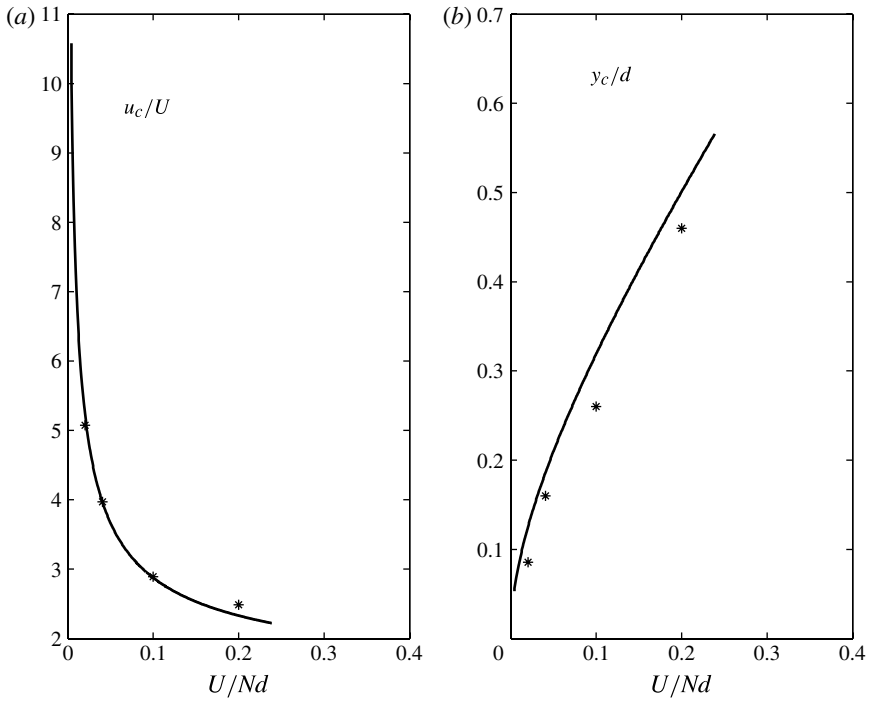

FIGURE 5. Solid curves: theoretical predictions of active layer velocity (a) and thickness (b) at the cylinder crest. Symbols show estimates of these quantities extracted from the numerical simulations shown in figure 1.

Figure 4 shows $\tilde{\mathscr{E}}_c$ as a function of y_{us} along with the square of the corresponding upstream Froude number F_{us} for the parameters N, d and U matching those in the flow with bulk Froude number $Fr_o = 0.04$.

Here $\tilde{\mathscr{E}}_c$ is equal to the critical value 3/2 for two distinct values of y_{us}. Both of these values are consistent with controlled flow at the cylinder crest. The smaller value has an upstream Froude number greater than 1 and therefore corresponds to a thin, fast supercritical layer that transitions to subcritical flow at the crest. Our interest here however is the asymmetric solution that transitions from subcritical flow upstream to supercritical downstream. This solution has $y_{us} \approx 0.28d$ for $Fr_o = 0.04$. We have now found the value of y_{us} (and the corresponding values g' and B for the specific case $Fr_o = 0.04$) consistent with a controlled layer that carries the excess transport required due to upstream blocking. We can therefore evaluate first the layer thickness at the crest using (4.6) and then solve for the average layer speed u_c from the condition that $F_c = 1$.

The theoretical crest conditions were computed as a function of $Fr_o = U/Nd$ and the results are shown in figure 5. The four specific numerical cases shown in figure 1 are also plotted. In these estimates, the layer thickness was defined to be the thickness of the layer with relative velocity greater than $1/e$ of the peak velocity in the layer. The layer speed was then taken to be the average speed in this layer. The theoretical predictions and the numerical estimates are in good agreement over the range of Fr_o tested.

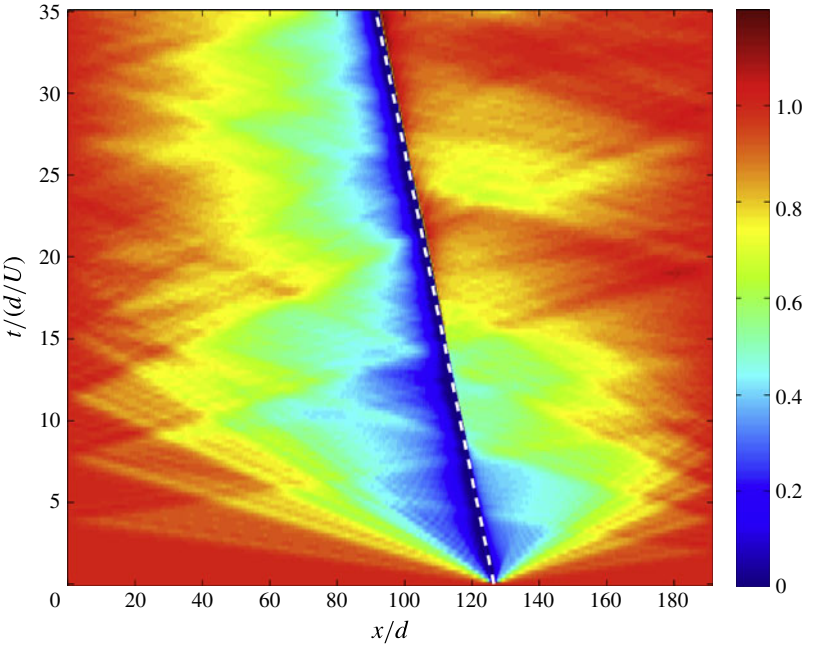

FIGURE 6. Horizontal speed relative to cylinder normalized by U at $z/d = 1/4$ for $Fr_o = 0.04$. The dashed line shows the position of the cylinder centre as a function of time.

5. Establishment of the quasi-steady flow

In these experiments, we chose a very long yet finite tank to match that of Browand & Winant (1972) and in our theoretical framework we ignore endwall effects and treat the flow upstream of the obstacle crest as steady. This simplifying approximation is, for the purposes of understanding dynamics of the active layer and its dependence on the external parameters U, N and d, well justified *a posteriori*.

Nevertheless, it is important to realize that the flow is never truly steady in towing tank experiments. Once the blocking zone extends upstream to an endwall, the vertical thickness of the blocked fluid must increase slowly with time, as noted by Browand & Winant (1972). If L is the distance from the cylinder to the upstream endwall and h is the thickness of the blocked flow measured from the centreline, the thickness increases at a rate $\mathrm{d}h/\mathrm{d}t = (h/L)U$. For these experiments we take $h \approx d$ and $L \approx 100d$ and so h increases $\sim$1 % of d over the characteristic time scale d/U. We note that these upstream boundary conditions are fundamentally different than imposing fixed profiles of velocity and density.

The finite distance to both endwalls can also generate unsteadiness if disturbances radiating from the cylinder reflect back into the interior of the domain. This effect can be seen in figure 6 which shows the normalized relative velocity at a height $z/d = 1/4$ for $Fr_o = 0.04$. It is clear that internal wave motions propagate both upstream and downstream at speeds much faster than the tow speed U. These signals reflect from the walls and then interfere with each other. Estimating phase speeds as $C_p = N\lambda/2\pi$ where λ is the vertical wavelength, the signals that reach the upstream wall between about $t/(d/U) = 7.5$ and 17.5 have vertical wavelengths of between $\sim 4d$ and $2d$. Waves with wavelengths smaller than $\sim d/8$ have phase speeds less than U and so

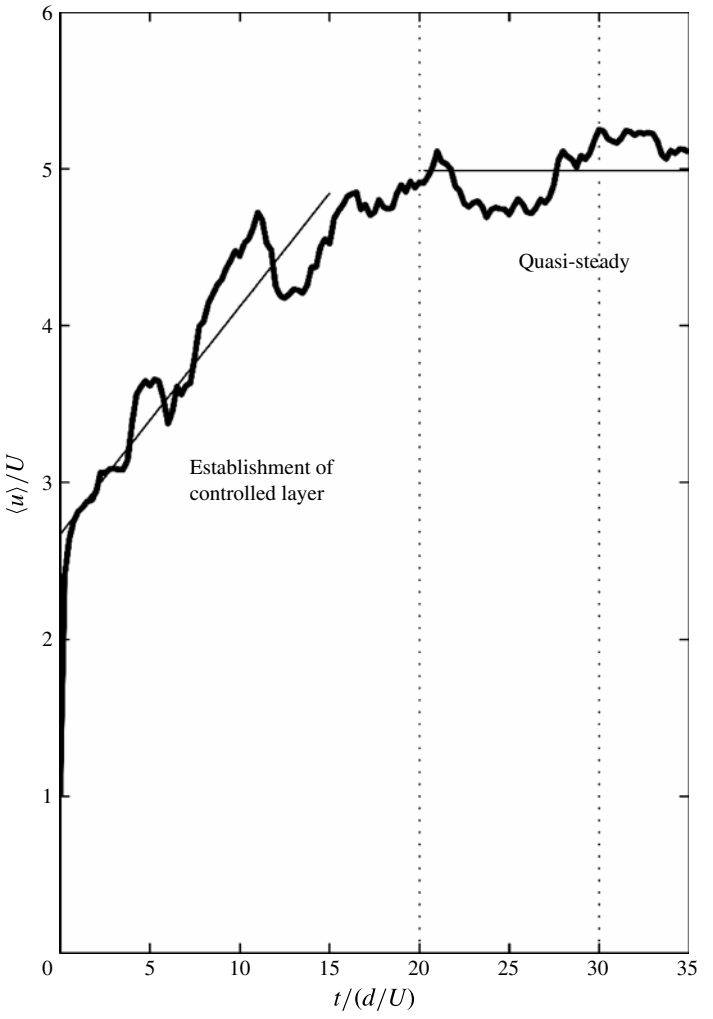

FIGURE 7. Horizontal speed relative to cylinder within active layer above cylinder crest for $Fr_o = 0.04$. The layer speed increases as the flow develops until about $t = 20d/U$ when a quasi-steady state is achieved. The best fits for uniform acceleration for $t \leqslant 15d/U$ and for steady flow for $t > 20d/U$ are also shown. Browand & Winant (1972) observed steady flow between $\sim$20 and $30d/U$ and began making measurements at $30d/U$. The numerical simulation results are analysed at $35d/U$.

cannot escape upstream. Nevertheless, the fastest waves that have multiple reflections in the finite sized domain have relatively little energy, $< 5\,\%$ of that associated with the tow speed, and thus do not greatly affect the much more energetic flow near the cylinder.

Even in the absence of endwall reflections, there is intrinsic unsteadiness due to the establishment of the downslope flow in the lee of the obstacle. As observed by Browand & Winant (1972), the flow initially separates close to the obstacle crest before the separation points move down the back of the cylinder. In their laboratory experiments, a steady state was observed between 20 and $30d/U$. figure 7 shows a similar result from the simulations. Shown is the average streamwise velocity in the

active layer above the crest as a function of dimensionless time. The flow develops until about $t = 20d/U$ at which time the average speed reaches an approximately steady value at 5 times the tow speed, with root mean square fluctuations of 3.3 %. Browand and Winant's recorded data after $t = 30d/U$ while in figures 1, 2 and 5 the flow was analysed at $t = 35d/U$. By this time the fully asymmetric flow has become established along with a favourable pressure gradient which prevents flow separation at the crest. This approach to an approximately steady state is not seen in towed experiments involving separated wakes, for example when towing sharp-crested obstacles (Castro & Snyder 1988) or in the numerical simulations of a moving vertical plate (Hanazaki 1989).

6. Discussion and conclusions

Continuously stratified flow past an obstacle can be understood and reasonably well described quantitatively in terms of a single-layer, reduced gravity model in which the layer transport q and reduced gravity g' are functions of the approach velocity U and the stratification N. Our theoretical framework describes the flow upstream of the obstacle and at its crest. The most important elements of the theory are the inclusion of upstream influence in the form of blocked flow beneath an energetically constrained level $\delta = U/N$ below the obstacle crest and the recognition that the flow above the active layer becomes dynamically uncoupled. These constraints determine, through continuity, the active layer transport. Combining these results with the requirement that the flow be asymmetric across the crest, i.e. hydraulically controlled, allows us to determine the upstream active layer thickness, the effective reduced gravity and thus all of the integral flow properties of the active layer. Although the experiments and simulations use a cylinder, the theory applies formally to any obstacle for which the hydrostatic approximation is appropriate. As for many hydraulics problems, we expect our conceptual framework to apply even for topography over which the flow is not strictly hydrostatic.

Downstream, the theory is not likely to be directly applicable as the flow is weakly unsteady (even at the relatively low Re considered here) and non-hydrostatic. Nonetheless, as the approach Froude numbers Fr_o decrease, the downstream Froude numbers in the lee increase because the thickness of the active layer and the effective g' decrease. This suggests that the dissipation and mixing in the jump will be more intense for decreasing Fr_o.

The theory constructed is an integral theory in which simplification is achieved by working with characteristic values representative of flows with continuously varying properties. Retaining nonlinearity is essential to the development. In the literature, perhaps the most closely related solution for continuously stratified flow over topography is due to Smith (1985). His solution also incorporates an isolating layer separating the downslope flow from that above. In contrast, however, the Smith solution neglects the blocked region and imposes the upstream flow to be the nearly uniform profile of Long (1955). It should be noted, however, that the velocity profiles shown in figure 2 are jet-like, reminiscent of Wood's (1968) self-similar solution for continuously stratified flow through a contraction. The actual velocity distribution of the upstream jet could be incorporated into the integral approach as a minor refinement of the development discussed here. Since the flow (see the differences in the velocity distributions upstream and at the crest in figure 2) is not self-similar as it is for the contraction, Wood's approach is not directly applicable here.

While the approach could be extended to include the effects of viscosity, it is remarkable how well the theory appears to work neglecting such effects, even for $Re = O(100)$. We can consider however, what the role of finite viscosity would be in these theoretically inviscid layered flows. Upstream, the theory postulates a thin stagnant layer that defines the bifurcating isopycnal and hence g'. This layer is bounded below by the fast moving jet with speed greater than U and above by the dynamically uncoupled flow with speed U. With finite viscosity, viscous stresses accelerate the stagnant layer, causing it to disappear. In the regime of the present simulations the stagnant layer is most pronounced near the crest and slightly downstream while it vanishes moving away from the obstacle upstream. At higher Re, we therefore expect the flow in the vicinity of the cylinder to be largely the same. However, immediately downstream of the cylinder, in the region of the internal hydraulic jumps, the Re effects will be more significant. In particular, at higher Re we expect shear instabilities and associated turbulent mixing to become apparent.

Acknowledgements

This work was supported by the National Science Foundation, grant number OCE-1061027. The authors thank C. Winant, R. Musgrave, A. de la Fuente and the reviewers for comments and discussion. This work was originally prepared for and presented at the special session honoring the career of F. Browand at the 7th International Symposium on Stratified Flows held in Rome, 24 August 2011.

REFERENCES

ARMI, L. 1989 Hydraulic control of zonal currents on a β plane. *J. Fluid. Mech.* **201**, 357–377.

BAINES, P. G. 1995 *Topographic Effects in Stratified Flows*. Cambridge University Press.

BROWAND, F. K. & WINANT, C. D. 1972 Blocking ahead of a cylinder moving in a stratified fluid: an experiment. *Geophys. Fluid Dyn.* **4**, 29–53.

CASTRO, I. P. & SNYDER, W. H. 1988 Upstream motions in stratified flow. *J. Fluid Mech.* **187**, 487–506.

DURRAN, D. R. & KLEMP, J. B. 1987 Another look at downslope winds. Part II: Nonlinear amplification beneath wave overturning layers. *J. Atmos. Sci.* **44**, 3402–3412.

ECHEVERRI, P., FLYNN, M. R., WINTERS, K. B. & PEACOCK, T. 2009 Low-mode internal tide generation: an experimental and numerical investigation. *J. Fluid Mech.* **638**, 91–108.

GRAEBEL, W. P. 1969 On the slow motion of bodies in stratified and rotating fluids. *Q. J. Mech. Appl. Maths* **22**, 39–54.

HANAZAKI, H. 1989 Upstream advancing columnar disturbances in two-dimensional stratified flow of finite depth. *Phys. Fluids* A **1**, 1976–1987.

LONG, R. R. 1955 Some aspects of the flow of stratified fluids. *Tellus* **7**, 341–357.

PRATT, L. J. & WHITEHEAD, J. A. 2008 *Rotating Hydraulics: Nonlinear Topographic Effects in the Ocean and Atmosphere*, p. 589. Springer.

SMITH, R. B. 1985 On severe downslope winds. *J. Atmos. Sci.* **42**, 2597–2603.

WINTERS, K., MACKINNON, J. & MILLS, B. 2004 A spectral model for process studies of rotating, density-stratified flows. *J. Atmos. Ocean Technol.* **21**, 69–94.

WOOD, I. R. 1968 Selective withdrawal from a stably stratified fluid. *J. Fluid. Mech.* **32**, 209–223.